AIP | Applied Physics Letters

Growth of ultra-uniform graphene using a Ni/W bilayer metal catalyst

Jae Hoon Yang, Jae Seok Hwang, Hyoung Woo Yang, A-Rang Jang, Hyeon Suk Shin, Jae-Eun Jang, and Dae Joon Kang

Citation: Applied Physics Letters **106**, 043110 (2015); doi: 10.1063/1.4907166
View online: http://dx.doi.org/10.1063/1.4907166
View Table of Contents: http://scitation.aip.org/content/aip/journal/apl/106/4?ver=pdfcov
Published by the AIP Publishing

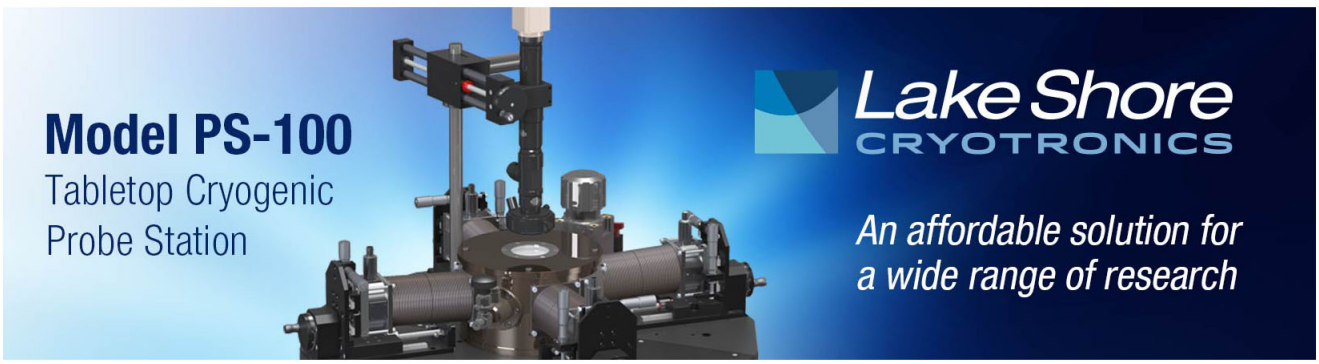

Growth of ultra-uniform graphene using a Ni/W bilayer metal catalyst

Jae Hoon Yang,[1,2] Jae Seok Hwang,[3] Hyoung Woo Yang,[1] A-Rang Jang,[4] Hyeon Suk Shin,[4] Jae-Eun Jang,[2] and Dae Joon Kang[1,a)]
[1]*Department of Physics, Sungkyunkwan University, Suwon 440-746, South Korea*
[2]*Department of Information and Communication Engineeing, Daegu Gyeongbuk Institute of Science and Technology, Daegu 711-873, South Korea*
[3]*Department of Energy Science, Sungkyunkwan University, Suwon 440-746, South Korea*
[4]*Department of Chemistry, Low Dimensional Carbon Materials Center, Interdisciplinary School of Green Energy, Ulsan National Institute of Science and Technology, Ulsan 689-798, South Korea*

(Received 11 November 2014; accepted 20 January 2015; published online 30 January 2015)

We investigated a bilayer catalyst system consisting of polycrystalline Ni and W films for growing mono-layer graphene over large areas. Highly uniform graphene was grown on Ni/W bilayer film with 100% coverage. The graphene grown on Ni/W bilayer film and transferred onto an insulating substrate exhibited average hole and electron mobilities of 727 and 340 $cm^2V^{-1}s^{-1}$, respectively. A probable growth mechanism is proposed based on X-ray diffractometry and transmission electron microscopy, which suggests that the reaction between diffused carbon and tungsten atoms results in formation of tungsten carbides. This reaction allows the control of carbon precipitation and prevents the growth of non-uniform multilayer graphene on the Ni surface; this has not been straightforwardly achieved before. These results could be of importance in better understanding mono-layer graphene growth, and suggest a facile fabrication route for electronic applications. [http://dx.doi.org/10.1063/1.4907166]

Graphene, a two-dimensional atomic crystal, has attracted considerable attention owing to its remarkable properties, such as being a zero-overlap semimetal with high electrical conductivity, displaying the half-integer quantum Hall effect,[1] and high carrier mobility.[2] As a result, it is considered a promising candidate for applications in various electronic devices, such as transistors[3–5] and transparent electrodes.[6,7] The use of graphene in viable electronic applications requires uniform deposition over large areas with a controllable number of layers. Various approaches, including mechanical exfoliation,[8] chemical exfoliation,[9] and chemical vapor deposition (CVD),[10] have been suggested for producing graphene. Among these, CVD has become the most promising approach for producing large-area graphene, using polycrystalline metals such as Ni,[10] Cu,[11] Ir,[12] Ru,[13] and Co[14] as catalysts. Ni and Cu have been extensively investigated as the most effective catalysts due to their low cost and large grain size. However, the fundamental limitation of utilizing Ni as a catalyst is that single- and few-layered graphene is obtained only over regions of a few to some tens of microns in size, and the graphene is not homogeneously distributed over the entire susucbstrate. The lack of control over the number of layers is partly attributed to the fact that segregation of carbon from the metal carbide upon cooling occurs rapidly within Ni grains and heterogeneously at grain boundaries. Although it is reported that the mono-layer graphene can be grown on Ni (111) single crystal in ultrahigh vacuum system, the cost of single-crystal catalyst is too expensive to facilitate the graphene applications.[15] Polymer films were also exploited as carbon sources to obtain graphene via a pyrolysis process, but with limited progress.[16,17] In contrast, the exceptional result of uniform deposition of high-quality monolayer graphene over large areas has been achieved on Cu foils. However, this graphene-growth process requires high temperatures, close to the melting temperature of Cu (~1084 °C), which roughen its surface due to sublimation of Cu. Furthermore, the weak interaction between graphene and Cu foil forms multiple graphene domains with different orientations.[18] Consequently, graphene grown on Cu may not be of the best quality. Recently, metal alloy films, such as Cu-Ni[19] and Ni-Mo,[20] have also been suggested for incorporating diffusing and precipitating carbon atoms into controlled formation of graphene. However, the alloys did not retain their pristine properties and showed different spatial concentrations of their constituent metal elements, resulting in synthesis of non-uniform graphene.

Herein, we report a growth of high-quality, large-area mono-layer graphene on Ni/W bilayer catalyst film. The key point of our approach is to take advantage of synergistic effects between constituent metals of the catalyst, in which the Ni thin film controls carbon precipitation, while the W thin film traps and controls excess carbon species dissolved in the Ni film during graphene synthesis. Growth of graphene using the CVD method based on a Ni/W bilayer catalyst film is highly beneficial for several reasons: (1) It allows large-scale synthesis of graphene of high uniformity and (2) the number of layers can be precisely controlled by changing the growth parameters.

To grow graphene on a Ni/W bilayer catalyst using CVD, a Ni/W film was prepared as follows: a polycrystalline W film of 100 nm thickness and a polycrystalline Ni thin film of 300 nm thickness were deposited in sequence onto a 300 nm-thick, thermally oxidized SiO_2 film on a Si substrate, using a laboratory-built e-beam evaporator. The as-prepared substrate was placed in a tubular quartz tube, heated, and

a)E-mail: djkang@skku.edu

held at 1000 °C for 25 min under H_2/Ar flow at a pressure of 250 mTorr. Graphene was grown by flowing a reaction-gas mixture (H_2:CH_4 = 10:30 sccm) at 650 mTorr for 3 min. The substrate was then rapidly cooled to room temperature under H_2 flow. Finally, single-layer graphene was formed on the Ni/W bilayer catalyst film. For comparison, graphene grown on Ni was also prepared as a reference sample. For subsequent characterization, as-grown graphene was transferred onto a SiO_2/Si substrate using the poly(methyl methacrylate) (PMMA)-mediated transfer method.[11] Carbidization of the W film was studied using X-ray diffraction (XRD) analysis (Bruker D8 Advance, Germany) with Cu-Kα radiation ($\lambda = 1.54056$ Å). Morphology of the graphene was examined by optical microscopy (Leica DX 105, Japan). Crystallinity and the number of graphene layers were evaluated by Raman spectroscopy (Renishaw RM1000-Invia, Germany) with an excitation wavelength of 514 nm. Confocal Raman spectroscopy mapping (WiTec CRM200, Germany) was also conducted with an excitation wavelength of 532 nm to visualize the uniformity and crystallinity of the graphene films. High-resolution transmission electron microscopy (HRTEM) (JEOL JEM2100F, Japan) was used to investigate the number of graphene layers and directly observe the tungsten carbide layer at the interface between the Ni and W films. Electrical properties of the graphene were investigated by fabricating back-gated field-effect transistors (FET): Ti/Au (10 nm/30 nm) was deposited using a laboratory-built e-beam evaporator to form drain and source electrodes, following conventional photolithography. After a metal deposition and lift-off process, a conduction channel of graphene ($\sim$4 μm wide, $\sim$5 μm long) was defined and etched by O_2 plasma-reactive ion etching. The electrical properties of the graphene were measured using a vacuum-probe station with a source-meter (Keithley 2612 Source-Meter, Japan) in a vacuum environment (30 mTorr) at room temperature.

Figure 1 compares graphene grown on Ni/W and Ni substrates. Figures 1(a) and 1(d) show optical microscopy images of the graphene films transferred from the Ni/W and Ni substrate, respectively. The graphene transferred from the Ni/W film showed a highly uniform color contrast, indicating uniform coverage (Figure 1(a)) On the other hand, graphene transferred from Ni showed a range of color contrasts, indicating different numbers of graphene layers (Figure 1(d)). We also used Raman spectroscopy to quantify the layers of graphene at the positions marked by circles in Figures 1(a) and 1(d); the corresponding Raman spectra are shown in Figures 1(b) and 1(e), respectively. From the position and intensity ratio of the G and 2D bands, we conclude that graphene grown on the Ni/W film was a perfect single-layer film. (Figure 1(b)). On the other hand, graphene grown on the Ni film is composed of a mixture of multi-layer and single-layer. The quality and morphology of graphene grown on Ni film was similar to typical results reported elsewhere.[10] Figures 1(c) and 1(f) plot the Raman intensities of the G and 2D bands around the marked region (orange rectangle) in Figures 1(a) and 1(d). It is obvious from the G/2D ratios that graphene grown on Ni/W film shows a highly uniform contrast (Figure 1(c)), while the graphene grown on Ni film contains mono-, bi-, and multi-layers (Figure 1(f)). This comparison suggests that graphene can be grown as a uniform single-layer on a Ni/W catalyst.

The graphene-growth mechanism using the bilayer catalyst system is depicted in Figures 2(a)–2(c). First, CH_4 gas is introduced into a furnace at sufficiently high temperature to supply energy to break carbon-hydrogen bonds in the presence of a catalyst (Figure 2(a)). Second, the source hydrocarbon molecules decompose at the surface of the Ni and diffuse into the Ni film. Diffused carbon atoms react with the W layer, resulting in formation of tungsten carbide at the interface between the Ni and W films (Figure 2(b)). Finally, during rapid cooling-down of the CVD system, carbon atoms precipitate and re-arrange on the Ni surface to form a graphene film (Figure 2(c)).

Figure 2(d) shows the XRD patterns of bare Ni/W and of graphene on Ni/W. The diffraction pattern of the bare Ni/W sample shows only Ni and W peaks. However, the diffraction pattern of graphene on Ni/W film also shows tungsten carbides, including WC and W_2C. These peaks indicate that hydrocarbon molecules diffused through the Ni layer and reacted with the W layer during graphene growth. This result is further supported by TEM analysis. Figure 2(e) shows a high-resolution TEM image of graphene on Ni/W;

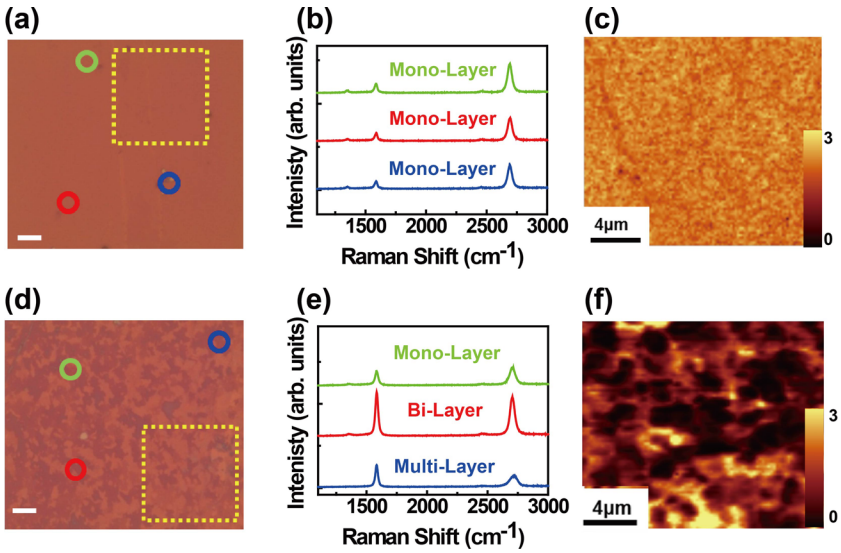

FIG. 1. Comparison of graphene grown on Ni/W ((a)–(c)) and Ni ((d)–(f)). (a) and (d) Optical images of graphene transferred onto 300 nm SiO_2/Si; the scale bar represents 5 μm. (b) and (e) Raman spectra from the regions marked by circles in frames (a) and (d). (c) and (f) Confocal Raman mapping of the intensity ratio of the G (1530–1630 cm^{-1}) and 2D (2600–2700 cm^{-1}) bands from the areas marked by orange rectangles in (a) and (d).

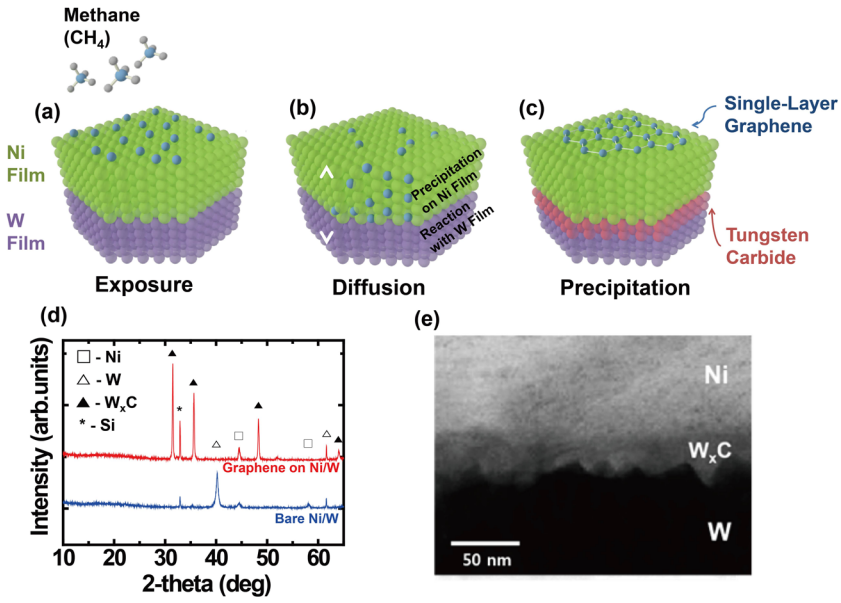

FIG. 2. (a)–(c) Schematic of the graphene-formation mechanism illustrating different process steps during growth. Shown are (a) surface-catalytic decomposition of the hydrocarbon source gas, (b) diffusion and precipitation into the metal bulk, and (c) reconstruction of carbon atom structures on the surface, resulting in single-layer graphene. (d) XRD patterns and (e) a cross-sectional TEM image of the bilayer catalyst revealing that a stable tungsten-carbide layer was formed at the interface between nickel and tungsten.

two stacked layers of Ni and W plus an intermediate layer are clearly observed. The different image contrasts in the three layers are induced by differing electron transmissions through the sample. Based on the XRD and TEM results, it is evident that carbon atoms diffused into the Ni layer were trapped in the underlying W layer. Thus, we believe that the kinetic behavior of the bi-layer metal catalyst was retained during graphene growth.

Transport measurements were used to evaluate electrical properties of the graphene grown on Ni/W. Figure 3 shows the optical microscopy image of a graphene FET and the device's transfer characteristics (I_d–V_g). The transfer characteristics were measured at a drain bias (V_d) of 0.1 V while varying the gate voltage in the range 0–40 V, as shown in Figure 3(b). The hole and electron mobilities were estimated from the linear regions of the transfer characteristic using the following equation:

$$\mu = \frac{1}{C_{ox}}\frac{\Delta\sigma}{\Delta V_g} = \frac{1}{C_{ox}WV_{sd}}\frac{\Delta I_d}{\Delta V_g} = g_m\frac{1}{V_{sd}WC_{ox}},$$

where C_{ox} is the specific capacitance of the SiO_2 dielectric layer, V_{sd} is the source-to-drain voltage, g_m is the transconductance, and μ is the field-effect carrier mobility. The hole and electron mobilities were calculated to be 727 and 340 $cm^2V^{-1}s^{-1}$, respectively (Figure 4(b)). In addition, its Dirac voltage (V_{Dirac}) was found to be ~20 V. The

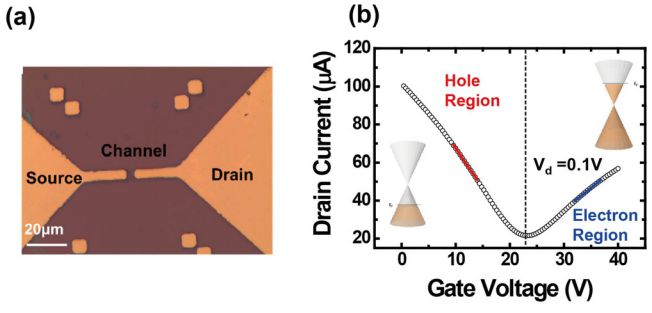

FIG. 3. Electrical characteristics of graphene FETs. (a) Optical image of a graphene FET device. (b) Transfer curve measured at $V_d = 0.1$ V.

asymmetric mobilities and the positive value of V_{Dirac} can be explained by different scattering cross-sections for different types of charge carriers, and by doping effects induced by charge-transfer doping of H_2O/O_2 molecules or metal-contact effects.[21]

To compare the uniformity of electrical properties (i.e., V_{Dirac} and carrier mobility) of graphene grown on Ni and on Ni/W, more than four hundred graphene FET devices were fabricated and characterized, as shown in Figures 4(a)–4(d). The V_{Dirac} of graphene grown on Ni/W varies between 15 and 30 V. In contrast, V_{Dirac} of graphene grown on Ni varies over a much larger range, between 7 and 58 V. As Filleter pointed out,[22] variations in graphene thickness affect its work function, resulting in a shift of V_{Dirac}. Further, the calculated carrier mobilities of graphene grown on Ni/W are distributed between 400 and 1500 $cm^2V^{-1}s^{-1}$, whereas the carrier mobilities of graphene grown on Ni are distributed between 200 and 4300 $cm^2V^{-1}s^{-1}$. Statistical histograms with Gaussian fits are shown in Figures 4(e)–4(h), indicating that graphene grown on Ni/W has average hole and electron mobilities of 730 and 341 $cm^2V^{-1}s^{-1}$, respectively, and a V_{Dirac} of 21 V at $V_d = 0.1$ V. In comparison, graphene grown on Ni had average hole and electron mobilities of 1400 and 540 $cm^2V^{-1}s^{-1}$, respectively, and V_{Dirac} of 29 V at the same V_d. The higher carrier mobilities observed for graphene grown on Ni can probably be ascribed to the screening effect induced by multilayer graphene from dangling bonds of SiO_2.[23] Furthermore, in CVD-grown graphene, hole mobility is typically higher than electron mobility because of contamination by water, polymer, or etchant residuals during the transfer process. Hence, graphene grown by CVD usually exhibits p-doped behavior. However, it is obvious that the histogram widths, as seen in of the Gaussian fits, are much wider for graphene grown on Ni, confirming the poor uniformity of graphene. These results demonstrate that the uniformity of graphene was greatly improved by using the Ni/W bilayer catalyst system. The uniformity of the carrier mobility and of V_{Dirac} of graphene affects the performance of electronic devices; the Ni/W bilayer catalyst system is more suitable for growing large-area, ultra-uniform graphene.

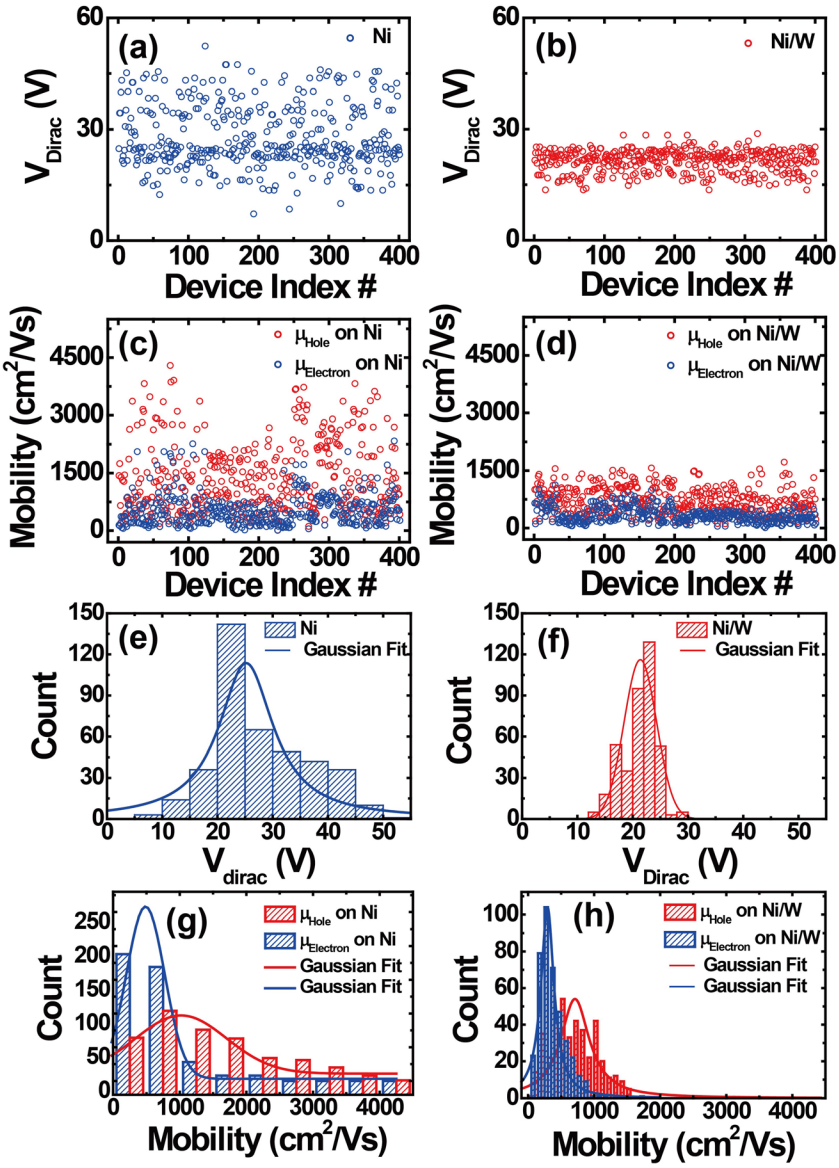

FIG. 4. Distribution analysis of (a) and (b) the Dirac voltage and (c) and (d) the carrier mobilities of FET devices fabricated from graphene grown on Ni/W (b) and (d) and Ni (a) and (c). Histograms of (e) and (f) the Dirac voltage, and (g) and (h) carrier mobilities, based on distributions (a)–(d).

Although the carrier mobility of graphene grown on Ni/W was found to be lower than on Ni, the process using Ni/W as catalyst would result in more effective and stable device applications.

We demonstrated the growth of ultra-uniform mono-layer graphene, utilizing a bilayer metal catalyst system consisting of Ni and W films. We also noted trapping of diffused carbon atoms upon carbidization; XRD and TEM results proved that diffused carbon atoms were trapped at the Ni-W interface as tungsten carbides. Raman spectroscopy and optical microscopy showed ultra-uniform, single-layer graphene. From these results, it is evident that graphene grown on Ni/W had an extraordinarily high uniformity with 100% coverage. We also investigated the electrical properties of graphene grown on Ni/W by fabricating a large sample of FETs and comparing them to FETs fabricated using graphene grown on Ni. This comparative study indicates that the Ni/W bilayer catalyst system can produce a large-area mono-layer graphene film that exhibits a highly uniform distribution of carrier mobilities and V_{Dirac}, to a greater degree than Ni alone. We believe that synergistic utilization of individual components of the bilayer catalyst may present a great opportunity not only for fundamental studies but also for industrial applications of ultra-uniform graphene.

This work was supported by the Center for BioNano Health-Guard funded by the Ministry of Science, ICT & Future Planning of Korea as the Global Frontier Project (HGUARD_2013M3A6B2078944) and Fundamental Technology Research Program through the National Research Foundation of Korea grants funded by Korean Government (No. 2014M3A7B4052201).

[1]Y. Zhang, Y.-W. Tan, H. L. Stormer, and P. Kim, Nature **438**, 201 (2005).
[2]E. Hwang, S. Adam, and S. D. Sarma, Phys. Rev. Lett. **98**, 186806 (2007).
[3]A. K. Geim and K. S. Novoselov, Nat. Mater. **6**, 183 (2007).
[4]G. Liu, W. Stillman, S. Rumyantsev, Q. Shao, M. Shur, and A. Balandin, Appl. Phys. Lett. **95**, 033103 (2009).
[5]Y.-M. Lin, A. Valdes-Garcia, S.-J. Han, D. B. Farmer, I. Meric, Y. Sun, Y. Wu, C. Dimitrakopoulos, A. Grill, P. Avouris *et al.*, Science **332**, 1294 (2011).
[6]X. Wang, L. Zhi, and K. Mullen, Nano Lett. **8**, 323 (2008).
[7]S. Pang, Y. Hernandez, X. Feng, and K. Mullen, Adv. Mater. **23**, 2779 (2011).
[8]Y. Hernandez, V. Nicolosi, M. Lotya, and F. M. Blighe, Nat. Nanotechnol. **3**, 563 (2008).

[9]K. S. Novoselov, A. K. Geim, and S. V. Morozov, Science **306**, 666 (2004).
[10]K. S. Kim, Y. Zhao, and H. Jang, Nature **457**, 706 (2009).
[11]X. Li, W. Cai, J. An, and S. Kim, Science **324**, 1312 (2009).
[12]J. Coraux, A. T. N'Diaye, M. Engler, and C. Busse, New J. Phys. **11**, 039801 (2009).
[13]P. Sutter, M. S. Hybertsen, and J. T. Sadowski, Nano Lett. **9**, 2654 (2009).
[14]H. Ago, Y. Ito, N. Mizuta, K. Yoshida, B. Hu, C. M. Orofeo, M. Tsuji, K.-I. Ikeda, and S. Mizuno, ACS Nano **4**, 7407 (2010).
[15]R. Addou, A. Dahal, P. Sutter, and M. Batzill, Appl. Phys. Lett. **100**, 021601 (2012).
[16]T. Takami, R. Seino, K. Yamazaki, and T. Ogino, J. Phys. D: Appl. Phys. **47**, 094015 (2014).
[17]H. J. Kwon, J. M. Ha, S. H. Yoo, G. Ali, and S. O. Cho, Nanoscale Res. Lett. **9**, 618 (2014).
[18]J. M. Wofford, S. Nie, and K. F. McCarty, Nano Lett. **10**, 4890 (2010).
[19]S. Chen, W. Cai, R. D. Piner, J. W. Suk, Y. Wu, Y. Ren, J. Kang, and R. S. Ruo, Nano Lett. **11**, 3519 (2011).
[20]B. Dai, L. Fu, Z. Zou, M. Wang, H. Xu, S. Wang, and Z. Liu, Nat. Commun. **2**, 522 (2011).
[21]D. B. Farmer, R. Golizadeh-Mojarad, V. Perebeinos, Y.-M. Lin, G. S. Tulevski, J. C. Tsang, and P. Avouris, Nano Lett. **9**, 388 (2008).
[22]T. Filleter, K. V. Emtsev, Th. Seyller, and R. Bennewitz, Appl. Phys. Lett. **93**, 133117 (2008).
[23]W. Zhu, C. Dimitrakopoulos, M. Freitag, and P. Avouris, IEEE Trans. Nanotechnology **10**, 1196–1201 (2011).